Microemulsion formulations for the transdermal delivery of testosterone

Rania M. Hathout[a,b], Timothy J. Woodman[b], Samar Mansour[a], Nahed D. Mortada[a], Ahmed S. Geneidi[a], Richard H. Guy[b*]

[a]Faculty of Pharmacy, Ain Shams University, Cairo, Egypt.

[b]Department of Pharmacy & Pharmacology, University of Bath, Bath, U.K.

Correspondence: Professor Richard H. Guy, Department of Pharmacy & Pharmacology, University of Bath, Claverton Down, Bath BA2 7AY, UK.

Tel: +44 (0) 1225 384901. Fax: +44 (0) 1225 386114. E-mail: r.h.guy@bath.ac.uk

Keywords: microemulsions – testosterone – ^{1}H-NMR – skin permeation – transdermal drug delivery.

Abstract

The objective was to develop a microemulsion formulation for the transdermal delivery of testosterone. Microemulsion formulations were prepared using oleic acid as the oil phase, Tween 20 as a surfactant, Transcutol® as co-surfactant, and water. The microemulsions were characterized visually, with the polarizing microscope, and by dynamic light scattering. In addition, the pH, conductivity (σ) and viscosity (η) of the formulations were measured. Moreover, differential scanning calorimetry and diffusion-ordered nuclear magnetic resonance spectroscopy were used to study the formulations investigated. Conductivity measurements revealed, as a function of the weight fraction of the aqueous phase, the point at which the microemulsion made the transition from water-in-oil to bicontinuous. Alterations in the microstructure of the microemulsions, following incorporation of testosterone, have been evaluated using the same physical parameters (pH, σ and η) and via Fourier-transform infra-red spectroscopy (FTIR), ^{1}H-NMR and ^{13}C-NMR. These methods were also used to determine the location of the drug in the colloidal formulation. Finally, testosterone delivery from selected formulations was assessed across porcine skin *in vitro* in Franz diffusion cells. The physical parameter determinations, combined with the spectroscopic studies, demonstrated that the drug was principally located in the oily domains of the microemulsions. Testosterone was delivered successfully across the skin from the microemulsions examined, with the highest flux achieved (4.6 ± 0.6 μg cm^{-2} hr^{-1}) from a formulation containing 3% w/v of the active drug and the composition (w/w) of 16% oleic acid, 32% Tween 20, 32% Transcutol® and 20% water. The microemulsions considered offer potentially useful vehicles for the transdermal delivery of testosterone.

1. Introduction

Testosterone is the major circulating male androgen (Leichtnam et al., 2006a). Its deficiency is usually associated with adverse effects on body composition, bone density, sexual function and mood, and may also increase cardiovascular risk. Numerous studies have demonstrated the benefits of testosterone replacement in overtly hypogonadal men. Amongst the several possible administration routes for testosterone replacement, transdermal delivery offers advantages over oral and intramuscular application in that both hepatic first-pass metabolism in the liver after oral administration, requiring high testosterone doses, and potentially painful injections combined with supra-physiological testosterone serum concentrations, are avoided. Moreover, the endogenous, circadian rhythm of testosterone secretion can be mimicked (Leichtnam et al., 2006b). The relatively low molecular weight (MW = 288) and moderate lipophilicity (log $P_{o/w}$ = 3.3; water solubility = 0.039 mg/ml at 37°C) (Okimoto et al., 1999) of testosterone are favourable factors for transdermal delivery. Gel formulations are already used clinically for the delivery of this hormone (e.g. Androgel®). However, these formulations have to be applied over large surface areas to achieve the target plasma levels and transfer of the drug to female partners has been recorded. While the approved transdermal patches (e.g. Testoderm® and Androderm®) avoid this problem, they have other drawbacks which significantly reduce patient acceptance and compliance (Leichtenam et al., 2006b). It follows that the development of alternative formulations for the transdermal delivery of testosterone remains a desirable goal.

Androgen replacement therapy should match normal physiological production (3-10 mg/day) of testosterone (Leichtnam et al., 2006b), corresponding to a target transdermal flux on the order of 1-10 μg cm^{-2} hr^{-1} for a 30 cm^2 patch. This objective has been achieved from semi-solid formulations and from transdermal patches (e.g. Androderm®) (Mitragotri et al., 1995; Marbury et al., 2003; Farahmand and Maibach, 2009). The maximum, passive flux of a drug across the skin is achieved when it is present in the applied formulation at its saturation concentration and, in a previous study, saturated solutions of

testosterone containing different percentages of ethanol, propylene glycol and water were assessed for the transdermal delivery of the drug and attained fluxes of ~1 μg cm^{-2} hr^{-1} (Leichtnam et al., 2006c). It is nevertheless possible to achieve the higher target fluxes of testosterone without using sophisticated technologies (e.g. electroporation, iontophoresis, sonophoresis, micro-perforation of the stratum corneum, etc.) via the incorporation of penetration enhancers into the formulation, or by increasing the drug's thermodynamic activity above unity using supersaturation. The limitation of the latter approach is stability, and the need to maintain the metastable state for a period sufficiently long so that an impact on drug transport is apparent (Leichtnam et al., 2006d). Consequently, the use of microemulsions, composed of excipients which include known penetration enhancers, was considered in this study. Single phase microemulsions are of interest as potential drug delivery vehicles due to their long term stability, ease of preparation, and considerable capacity for solubilisation of a variety of drug molecules (Malmstein, 1999; Lawrence and Rees, 2000). They are thermodynamically stable and optically isotropic, transparent, colloidal systems consisting of water, oil and amphiphiles (surfactant, usually in combination with a cosurfactant) (Stilbs et al., 1983; Langevin, 1988). When a sufficient amount of an appropriate surfactant is added to solubilise oil and water completely, single phase systems (Winsor IV microemulsions) are formed (Winsor, 1948). Four-component systems of surfactant, cosurfactant, oil, and water have many important features and are the most studied microemulsions. Moreover, interest in using non-ionic tensioactives, both as surfactant and as cosurfactant, is increasing due to their high stability, low toxicity, low irritancy and biodegradability (Malmstein, 1999; Lawrence and Rees, 2000). Transcutol® is a powerful solubilising agent, the use of which in dermal and transdermal delivery has been examined in some detail, due to its non-toxicity, biocompatibility with the skin, miscibility with polar and non-polar solvents and optimal solubilising properties for a number of drugs (Barthelemy et al., 1995). Mono-unsaturated fatty acids, such as oleic acid, have received attention as effective penetration enhancers (Golden et al., 1987). The aim of this work is the development of a microemulsion

formulation for the transdermal delivery of testosterone using oleic acid as the oil phase, Tween 20 as a surfactant, Transcutol® as co-surfactant, and water.

2. Materials and Methods

2.1. Materials

Oleic acid, polyethylene 20 sorbitan monolaurate (Tween20®), polyethylene 40 sorbitan monopalmitate (Tween40®) and polyethylene 80 sorbitan monooleate (Tween80®) (Sigma-Aldrich, Gillingham, UK), diethylene glycol monoethyl ether (Transcutol®) (Gattefosse, Lyon, France), testosterone (Sigma, St.Louis, MO, USA), acetonitrile, ethanol (HPLC grade) (Fisher Scientific, Loughbrough, UK), sodium chloride, potassium chloride, sodium phosphate (monobasic) and potassium phosphate (dibasic) (Acros Organics, Geel, Belgium), deuterated water (Cambridge isotope laboratories, Andover, MA, USA) and Parafilm® (Pechiney plastic packaging company, Chicago, IL, USA). All aqueous solutions were prepared using high-purity deionized water with conductance less than 1 μS cm^{-1} (18.2 MΩ.cm) (Barnstead Nanopure Diamond, Dubuque, IA, USA).

2.2. Methods

2.2.1. Construction of pseudo-ternary phase diagrams

To determine the concentration ranges of components over which microemulsions would form, pseudo-ternary phase diagrams were constructed using the water titration method at ambient temperature (25°C) (Chen et al., 2004). Phase diagrams were prepared with different surfactants and different weight ratios of surfactant to co-surfactant. For each phase diagram, the ratios of oleic acid to the mixture of surfactant and cosurfactant were varied as 1:9, 2:8, 3:7, 4:6, 5:5, 6:4, 7:3, 8:2, 9:1. The mixture of oil, surfactant and cosurfactant was diluted with water, under moderate stirring. After equilibration, the mixtures were assessed visually as either one-phase microemulsions or two-phase mixtures. Turbidity was considered an indication of phase separation. Every sample that remained transparent and homogenous after vigorous vortexing was assigned to a monophasic area in the phase diagram (Garti et al., 2000).

2.2.2. Polarized light microscopy

To verify the isotropic nature of microemulsions, samples were examined using cross-polarized light microscopy (Olympus BX51 U-AN 360, Tokyo, Japan). A drop of sample was placed between a coverslip and a glass slide and observed under cross-polarized light. Isotropic material, such as a microemulsion, in contrast to anisotropic liquid crystals, will not interfere with the polarized light (Friberg, 1990) and the field of view remains dark.

2.2.3. Water solubilisation parameters

One of the goals of this work was to incorporate a large amount of water and oil into the microemulsions. The total monophasic area has been used as a solubilisation parameter (Fanun, 2008), and it is the sum of all one-phase cross-sectional areas in the tetrahedral phase diagram. The water and oil solubilization was estimated as the monophasic area (A_T) of the relevant pseudo-ternary phase diagrams. It is also well documented that the water solubilization capacity of different amphiphilic systems should be strictly compared at optimal solubilisation capacity. Because the maximum solubilisation of water appears in some systems on different water dilution lines (a line in the phase diagram beginning with a mixture of oil/surfactant/cosurfactant at a fixed ratio, which is diluted with water), it is common to state the maximum solubilisation of water (W_m) on the dilution line where maximum solubilisation was obtained (see Figure 1).

2.2.4. Particle size measurements

The particle size and the polydispersity of the microemulsions were determined using dynamic light scattering (Malvern Zetasizer , Malvern, Worcestershire, UK) assuming a viscosity of 0.05 PaS. The scattering intensity data were obtained from pre-filtered (0.45 μm) microemulsions (Delgado-Charro et al., 1997). The samples were loaded into cuvettes having a volume of 1 cm^3 in a thermostated chamber at 25°C. Triplicate measurements were made.

2.2.5. Electrical conductivity measurements

Electrical conductivity (σ) of oleic acid/Tween20/Transcutol®/water microemulsions was measured using a conductometer (Metrohm 712, Herisau, Switzerland) at a frequency of 94 Hz. The measurements were performed in triplicate at 25 (±1) °C. The electrode material was graphite and the cell constant was 0.965 cm^{-1} (±1.5%). The electrode was dipped in the microemulsion sample until equilibrium was reached and the reading became stable. Reproducibility was excellent. The conductivity cell constant was calibrated using standard KCl solutions and checked no less than three times during the course of the work.

2.2.6. Differential scanning calorimetry (DSC)

The thermal behaviour of water can be a helpful and rapid means with which to understand the microstructure of microemulsions (Liu et al., 2009). DSC measurements were carried out as follows: microemulsion samples (6-18 mg) were weighed into aluminium pans and immediately pressure sealed; measurements were performed in the cooling (exothermic) mode on an EX star / SII 7020 high sensitivity DSC (SII Nano Technology Incorporation, Tokyo, Japan) equipped with an automatic liquid nitrogen cooling unit; the samples were equilibrated at 25°C for 5 minutes, then gradually cooled by liquid nitrogen at a predetermined rate from ambient to -60°C at a constant scanning rate of 10C° / min. An empty pan was used as a reference. Nitrogen with a flow rate of 0.3 L/min was used as purge gas.

2.2.7. Diffusion-ordered spectroscopy (DOSY)

All PGSE (Pulsed Gradient Spin Echo) measurements were determined using a Varian Mercury 400 MHz spectrometer (Varian Inc., Palo Alto, CA, USA) equipped with a 4-nucleus auto-switchable probe, using the Dbppste pulse sequence, at 25°C, without spinning the sample. Gradient strength (G) was varied over 15 spectra, which were acquired with 32K data points, over a spectral width of 5 MHz, with a relaxation delay of 5 seconds and processed with line broadening of 1 Hz. Since the samples were essentially highly concentrated, only 4 transients were recorded for each gradient strength. For each

component, a characteristic peak was selected such that in the ^{1}H-NMR of the micro-emulsion the peak was clearly separate from all other peaks. For water, this corresponds to a broad peak at 4.69 ppm. For oleic acid, the triplet between 0.98 and 1.05 ppm was used for determining D_o^{oil} taking an average of the values obtained for the three lines in the spectrum. Self diffusion coefficients for pure water (D_o^{water}) and neat oil (D_o^{oil}) at 25°C were determined. Using the same conditions, *DOSY* analysis of the water and oil in the microemulsions was performed using the peaks identified from the pure components.

2.2.8. pH measurements

The pH of the selected oleic acid/Tween20/Transcutol®/water microemulsions was measured using a Thermo Orion pH meter (Thermo Fisher Scientific, MA, USA). Triplicate measurements were made.

2.2.9. Rheological measurements

Dynamic viscosity (η) was determined at 20°C with a Bohlin rheometer (Bohlin Instruments, Gloucestershire, UK), using cone (4 cm diameter, 4 grad. angle) and plate geometry. Shear rates of between 0.1 and 5 sec^{-1} were used. All samples were measured in triplicate.

2.2.10. Fourier-transform infrared spectroscopy (FT-IR)

FT-IR spectra of the microemulsions, with and without drug incorporation, were recorded on a Perkin-Elmer (RX1) FTIR spectrometer (Perkin-Elmer, Waltham, MA, USA) using NaCl plates, in the frequency range 4,000–350 cm^{-1} with 64 scans and 4 cm^{-1} spectral resolution.

2.2.11. ^{1}H-NMR and ^{13}C-NMR

NMR measurements were performed at 25°C on Varian Mercury 400 MHz using D_2O as internal locking agent.

2.2.12. Preparation of testosterone microemulsions

Testosterone was dissolved gradually in an oleic acid/Transcutol® mixture. Magnetic stirring was used. After complete solubilisation, Tween20 was added and the mixture was then diluted with water under moderate stirring.

2.2.13. Alteration of microemulsion microstructure after drug loading

Microstructure alterations in the microemulsions, following incorporation of testosterone (1% and 3% w/v), were evaluated via physical measurements of pH, σ and η, and with FTIR, ^{1}H-NMR and ^{13}C-NMR. These results were also used to determine the location of the drug in the colloidal formulation.

2.2.14. Skin

Dorsal porcine skin was obtained from animals slaughtered at a local abattoir and dermatomed to a thickness of 740 μm. The skin was stored (for a period of no more than one month) at -20°C until use.

2.2.15. In vitro permeation experiments

Skin was defrosted, cut into circular sections and mounted with the stratum corneum uppermost in Franz-type diffusion cells (Permegear, Hellertown, PA, USA). The receptor volume was 7.5 ml and the diffusional area was 1.77 cm^2. Before starting the transport experiment, the receptor solution was filled with phosphate buffered saline (PBS) at pH 7.4 and the skin surface was covered with 1 ml of the same solution. The cells were equilibrated in a water bath at 37°C for 1 hour. The receptor was magnetically stirred. Subsequently, the PBS in the donor was replaced by 2 ml of microemulsion containing 1% w/v testosterone and the compartment was covered with Parafilm®. A 0.5 ml sample of the receptor fluid was collected at 2, 4, 6, 8, 10, 24, 28 and 30 h and immediately replaced with fresh solution. All samples were filtered using 0.45 μm Nalgene® Millipore syringe filters (Thermo Fisher Scientific, Waltham, MA, USA) prior to analysis. All the experiments were performed in triplicate.

2.2.16. High performance liquid chromatography (HPLC) assay for testosterone

For isocratic chromatography, a Phenomenex® C18, 5 µm, 50×4.6 mm column (Phenomenex, Torrance, CA, USA) was used at 25°C. UV detection at 241 nm was performed using the UV detector of a Shimadzu 2010 EV liquid chromatograph mass spectrometer (Shimadzu, Kyoto, Japan) together with a Spectra Serie P 100 HPLC-pump (Thermo separation products, Riviera beach, FL, USA). A 60:40 (v/v) degassed mixture of acetonitrile and water was used as the mobile phase. At a flow rate of 1 ml/min, the retention time of testosterone was 1.3 ± 0.3 min. Unknown testosterone concentrations were calculated against known standards. The quantitation limit of the assay was 0.1 µg/ml; when a solution of drug at that concentration was injected on six separate occasions, the HPLC response had a coefficient of variation (CV) of 0.24%. Repeating this experiment on a different day resulted in essentially identical results, this time with a CV of 0.25%. The method was therefore considered repeatable and reproducible.

2.2.17. Data Analysis

The permeation results were expressed as the cumulative amount of drug transported across the skin barrier per unit area (Q) as a function of time (t). Each permeation curve was fitted to the appropriate solution (Eq. 1) of the non-steady state diffusion equation (Fick's second law (Friend, 1992)), which assumes the boundary conditions (a) that there is no depletion of the drug in the donor compartment over the course of the experiment, (b) that the receptor phase provides "sink conditions", and (c) that at t = 0, there is no drug in the skin (Sekkat et al., 2004). That is,

$$Q = \{KH\}C_{veh}[(\frac{D}{H^2}t - \frac{1}{6} - \frac{2}{\pi^2}\sum_{n=1}^{\infty}\frac{(-1)^2}{n}\exp(\frac{-Dn^2\pi^2.t}{H})] \quad (1)$$

where C_{veh} is the drug's concentration in the donor solution and K is its SC-microemulsion partition coefficient; D is the diffusivity of the drug in the SC of thickness H.

The fitting procedure used a commercial software package (Prism, Version 5, GraphPad Software, San Diego, CA, USA), running on a personal computer, and enabled the drug's characteristic

partitioning (KH) and diffusivity (D/H^2) parameters to be deduced. In turn, the conventional permeability coefficient (k_p) of the drug across the skin was found:

$$k_p = (KH) \times \left(D / H^2 \right) = \frac{K.D}{H} \quad (2)$$

together with the estimated steady-state drug flux J_{ss}

$$J_{ss} = k_p \times C_{veh} \quad (3)$$

2.2.18. Final experiments

In a last set of experiments, the drug concentration was increased from 1% to 3% w/v in the microemulsion which best delivered testosterone across the skin and the *in vitro* study was repeated. Physical characterization and spectroscopic analyses were conducted and compared to the corresponding unloaded and 1% w/v microemulsion.

3. Results and discussion

3.1. Solubilisation parameters for different microemulsions

The isotropic and low-viscosity region is presented in the phase diagram (Figure 1) as the one-phase microemulsion region (1Φ). The remainder of the phase diagram represents the turbid region, represented as multiphase (MΦ), conventional emulsions. These results were confirmed using polarized light microscopy. The total monophasic region (A_T) of the system oleic acid/Tween20/Transcutol®/water was 16.9 (±2.9) %.

3.2. Effect of surfactant chain length on microemulsion formation

The surfactants considered were Tween20, Tween40 and Tween80, and the effect of chain length on A_T, W_m and S_m are presented in Figure 2. The highest A_T and W_m, and the lowest S_m, were observed with Tween20 (C-12) which has the shortest chain length, the highest hydrophilicity (HLB 16.7), and the greatest ability to incorporate water (Thevenin et al., 1996). Furthermore, Tween20 has the lowest dynamic viscosity (400 cp) compared to that of Tween40 (500 cp) and Tween80 (425 cp). It is worth noting that Tween80 had higher A_T and W_m than Tween40 presumably due to its unsaturation at C-9 which increases its HLB. The compatibility between the individual components is an important factor with respect to the formation of microemulsions (Hou and Shah, 1987; Bayrak and Iscan, 2005a; Bayrak and Iscan, 2005b). From the results obtained here, together with the established relationship between surfactant alkyl chain length and skin penetration enhancement ability (Zaslavsky et al., 1978; Walters et al., 1981; Florence et al., 1983; Lopez et al., 2000), Tween20 was selected for further investigations.

3.3. Effect of the surfactant/cosurfactant ratio on microemulsion formation

The mixing ratios of surfactant to Transcutol® considered were 1:3, 1:1 and 3:1. The effect on A_T is presented in Figure 3. The 1:1 ratio gave the highest value: 16.9 (± 2.9) %.

3.4. Particle size

Dynamic light scattering revealed that the average droplet diameter for all microemulsions investigated was 10-13 nm (Table 1). A small droplet size provides increased stability against sedimentation, flocculation, and coalescence (Cho et al., 2008).

The internal-phase ratio (Ø) was calculated (Lissant, 1974) for each formulation (Table 1). For a W/O microemulsion system,

$$Ø_w = (V_{H2O}+V_{surf+cosurf})/ V_{tot} \quad (4)$$

while, for an o/w microemulsion,

$$Ø_o = (V_o+V_{sur.+cosurf})/ V_{tot} \quad (5)$$

where *V* represents the volume of the phase(s) indicated by the subscript. The results in Table 1 show that the droplets occupy 27-90% of the w/o or o/w microemulsions investigated. Because the partitioning of surfactant/cosurfactant between the droplets and the continuous phase is unknown, the calculated phase volumes are apparent values rather than absolute (Baroli et al., 2000). Assuming that microemulsion droplets behave like rigid spheres, stronger hydrodynamic interactions between them are expected as their number increases (Lissant, 1974), and aggregates may be formed. Maximum droplet aggregation is anticipated for the largest Ø values and this was confirmed by the high polydispersity index (recognising, of course, that values of polydispersity approaching 1 indicate that particle size estimates come with considerable uncertainty).

3.5. Electrical conductivity measurements (σ)

It has been previously demonstrated that strong correlations exist between a microemulsion's structure and its electroconductive behaviour (Clausse et al., 1987a). Conductimetry is therefore a useful tool with which to assess aspects of a microemulsion's properties (Clausse et al., 1987b). In Figure 1, Line L20 starting at 20% v/v oil to 80% v/v surfactant/co-surfactant represents a wide range of stable microemulsions containing increasing amounts of water. Figure 4a shows the influence of water content on the electrical conductivity of oleic acid/Tween20/Transcutol®/water compositions along the line L20.

As the volume percentage of water increases, the electrical conductivity increases. In the so-called percolation model, the conductivity remains low up to a certain volume fraction of water (Fanun, 2008). If a dramatic change in conductivity at a given water volume fraction (Φ) is recorded, then a phase inversion from reverse swollen micelles (w/o) to direct micelles (o/w) is suggested (Thevenin et al., 1996). This transition is explained by the emergence of bicontinuous structures which possess ultralow interfacial tension. Conductivities >1 μS/cm have been reported to be indicative of bicontinuous or solution-type microemulsions, where the presence of water in the continuous pseudo-phase leads to measurable conductivity (Krauel et al., 2005; Graf et al., 2008). These dynamic structures include water and oil pseudo-domains which rapidly exchange (Baker et al., 1984). In the presence of these structures, the conductivity is comparable to that of electrolyte solutions and decreases with decreasing water content. Under these conditions, the conductivity drops sharply by more than one order of magnitude (Lagourette et al., 1979). The conductivity of w/o microemulsions are on the order of 10^{-6} S/m, i.e., much higher than those typical of apolar solvents (10^{-16}-10^{-12} S/m) (Giustini et al., 1996).

Water-in-oil droplets, below a critical water volume fraction (Φ_c) are isolated from each other and are embedded in the non-conducting, continuum oil phase; hence, they contribute very little to the electrical conductance. However, as the volume fraction of water reaches Φ_c, contact between these conductive droplets occurs and results in the formation of clusters. The number of such clusters increases very rapidly above this so-called percolation threshold, giving rise to the observed changes in electrical conductivity. The electrical conductivity increase above Φ_c has been attributed both to ion hopping from droplet to droplet within clusters, to transfer of counter ions from one droplet to another through water channels during sticky collisions, and to the transient merging of droplets (Mathew et al., 1988). The threshold depends on interactions between droplets, which control the duration of the collision and the degree of interface overlap, and hence the probability of hopping or merging. Increasing conductivity

requires attractive interactions and Φ_c decreases as the strength of these inter-droplet interactions increases (Safran et al., 1985).

In these systems, conductivity follows a universal law independent of the physical properties of the medium and, near the percolation threshold (Bisal et al., 1990),

$$\sigma = (\Phi - \Phi_c)^t \quad (6)$$

where σ is the conductivity, Φ is the dispersed water volume percentage, Φ_c is the dispersed volume percentage at the percolation threshold, and t depends on the system dimensionality (t = 1.5-1.6 for a 3-dimensional system) (El-Laithy, 2003).

To test the validity of the percolation theory, (log σ)/t and d(logσ)/dΦ were plotted as a function of Φ (Figure 4). For the system oleic acid/Tween20/Transcutol®/water, the x-axis intersect in Figure 4b indicates that Φ_c = 2.8 (±0.2) μS/cm, while Figure 4c shows a maximum corresponding to Φ_c = 3 (±0.1) μS/cm. Incorporation of the drug had no significant effect on the conductivities of the microemulsions A to F (Table 3).

3.6. Differential scanning calorimetry

The cooling curves of all pseudo-ternary mixtures investigated (Table 2) show one exothermic peak (Figure 5). With increasing water fraction, the peak shifts towards higher temperatures. The changes tend towards the freezing behaviour of pure water as shown by the reference measurement with its maximum at about -17°C. Therefore, the exothermic event represents the freezing of super-cooled water (Broto and Clausse, 1976; Podlogar et al., 2004). The decreasing water fraction goes hand-in-hand with an increase in the amount of surfactant and this leads to more strongly bound water molecules being needed to hydrate the polar head groups. Correspondingly, a decrease in the freezing temperature can be anticipated and the presence of non-freezing water is therefore likely (Yaghmur et al., 2002). In this context, a small broadened peak at very low temperatures (below -30°C) has been suggested to be either internal water or water that is interacting strongly with the surfactants (Podlogar et al., 2004;

Podlogar et al., 2005). The behaviour might be expected in the system containing 5% water. Since the other peaks are also broadened, but show maxima at more than -30°C , these mixtures may be demonstrating a structural change towards bicontinuous microemulsions. Similar deductions can be made from the electrical conductivity experiments.

3.7. DOSY measurements

Diffusion-ordered nuclear magnetic resonance (NMR) spectroscopy (DOSY) is a powerful technique that enables discrimination among molecular species using apparent translational diffusion coefficients. A DOSY experiment performed on a mixture results in a two-dimensional spectrum which displays conventional NMR spectral information (chemical shifts) in one dimension and the apparent self diffusion coefficient in the other. This apparent self diffusion coefficient is calculated by measuring the decay obtained of the spin echo spectra using pulsed field gradients (Liu et al., 2009). The relative diffusion coefficient D/D_o, of water and oil in the nanodroplets versus the diffusion coefficient in a solution is used to evaluate the self-diffusion data in terms of microstructure. The D_o^{water} determined using the peak at 4.69 ppm was 20.3 x 10^{-10} m^2 s^{-1}, which is consistent with literature values (Ghi et al., 2002). The value of D_o^{oil} was 0.33 x 10^{-10} m^2 s^{-1}. Relative diffusion coefficients of the water and the oil were obtained by dividing water and oil diffusion coefficients in the microemulsion by those in the neat phases. It was previously documented that discrete particles of the slowly diffusing solvent are indicated if the D/D_o values of water and oil differ by more than one order of magnitude; alternatively, if the D/D_o values of water and oil are of the same order of magnitude, a bicontinuous structure is implied (Libster et al., 2006). The selected microemulsions (Table 2) containing 5-23% aqueous phase had relative diffusion coefficients for water and oleic acid of the same order of magnitude as shown in Figure 6. This would suggest a bicontinuous microstructure in agreement with the DSC and conductivity measurements reported above.

3.8. pH measurements

The pH decreased significantly ($p < 0.05$ using a one-way ANOVA and Bonferroni's post test) from 5.23 to 4.56 for the selected microemulsion formulations (Table 2) as the water concentration progressively increased from 5 % to 23%. At higher water content, the ionization of the organic acid present increases, releasing more protons into the solution and reducing the pH (Spernath et al., 2006). Incorporation of the drug caused no significant change in the pH (Table 3). Nevertheless, the pH values observed are considered physiologically acceptable.

3.9. Rheological measurements

Newtonian flow was suggested for the microemulsions investigated as the viscosity remained constant at different shear rates. The dynamic viscosity of the microemulsion formulations ranged from 0.047 to 0.061 Pa s. ANOVA and Bonferroni's post test showed that there was no significant difference at $p < 0.05$ between any of the measured viscosities. The viscosity of a microemulsion is a function of the surfactant, water and oil components and their concentrations (Yuan et al., 2008). The viscosity is governed by two opposing effects: increasing the water content is expected to lower the viscosity while decreasing the amount of surfactant and co-surfactant increases interfacial tension between oil and water, decreases interfacial area, increases the size of the internal domains and therefore increases viscosity (El Maghraby, 2008). Adding the drug caused no significant increase ($p < 0.05$) in viscosity (Table 3).

3.10. FTIR, ^{1}H-NMR and ^{13}C-NMR spectroscopy

The O-H stretching frequency in the infrared can be used to measure the strength of a hydrogen bond. The stronger the H-bond, the lower the vibration frequency and the broader and more intense the absorption band (Williams and Fleming, 1996).

The O-H absorbance of microemulsions A to F occurred at higher frequencies than pure water (3400 cm^{-1}) (Table 3) due to H-bond interactions between water, the surfactant and the co-surfactant. These bonds are weaker than intermolecular H-bonds in water alone. As the water content in the microemulsions (ME A to ME F) increased, the O-H absorbance shifted to lower frequencies.

Incorporation of the drug had a negligible effect on the O-H stretching frequency (Table 3). In other words, the drug did not influence the water-surfactant interface (Mehta et al., 2008), consistent with its probable location in hydrophobic domains and its low aqueous solubility. This would suggest no alteration in the microemulsion microstructure with drug incorporation, in agreement with the conductivity, pH and rheological measurements.

The ^{1}H-NMR and ^{13}C-NMR spectra and peak assignments to different groups of the microemulsion components are presented in the Supplementary Information. The changes in chemical shifts of the protons in the distinct functional groups (CH_3, CH_2CH and CH) of oleic acid after drug incorporation were the highest. These results were confirmed using ^{13}C-NMR, where C=C and -CH_3 carbons scored the highest shifts. These results are consistent with the physical characterisation and FTIR spectroscopy findings, and confirm that testosterone is found primarily in the oil domain of the microemulsions.

3.11. In vitro permeation

Figure 7 shows the permeation profiles of testosterone from the selected microemulsion formulations and the corresponding fitting of the data to Fick's second law. Drug partitioning (KH) and diffusivity (D/H^2) parameters, estimated permeability coefficients (k_p) and steady-state fluxes (J_{ss}) for each formulation are summarized in Table 4.

Different mechanisms have been proposed to explain the enhanced transdermal delivery of drugs using microemulsions: via increased thermodynamic activity of the drug, through the action of microemulsion ingredients as permeation enhancers, and because of increased skin hydration (Williams

and Barry, 2004). All these possibilities are supported in some way by the results (Rhee et al., 2001): testosterone flux increased with increasing water content of the microemulsion, consistent with a higher thermodynamic activity of the drug and a greater level of skin hydration. Equally, when the level of the known penetration enhancer, oleic acid, fell below 16 %, the flux of testosterone was reduced.

Increasing the loading dose of drug is an effective method to improve the skin permeation rate (Zhao et al., 2006). Figure 8 demonstrates this principle for testosterone in microemulsion E with the drug flux increasing from 1.40 (± 0.44) to 4.63 (± 0.61) μg cm^{-2} h^{-1} as the loading was raised from 1% to 3% w/v.

4. Conclusion

Microemulsions for the transdermal delivery of testosterone have been developed and fully characterised and shown to achieve percutaneous absorption rates of the drug consistent with effective clinical treatment. Further work is required to determine whether a microemulsion may ultimately be incorporated into a transdermal patch, and take advantage of the favourable delivery rate as well as the lower skin irritation potential which has been reported for formulations of this type. Alternatively, one might envisage a more conventional 'unit-dose' system of a microemulsion, such as a gel, designed for application over a specific and controlled skin area (e.g., the backs of the hands); in this case, it may be possible to adjust downwards the level of penetration enhancer with a view to mitigating further any irritation effects.

5. Supplementary information

^{1}H-NMR chemical shift data for microemulsions E and F. ^{13}C-NMR chemical shift data of microemulsion F. ^{1}H-NMR and ^{13}C-NMR spectra and assignment of peaks for microemulsion F.

References

Baker, R.C., Florence, A.T., Ottewill, R.H., Tadros, T.F., 1984. Investigations into the formation and characterization of microemulsions. 2. Light-scattering, conductivity and viscosity studies of microemulsions. J. Colloid Interface Sci. 100, 332-349.

Baroli, B., Lopez-Quintela, M.A., Delgado-Charro, M.B., Fadda, A.M., Blanco-Mendez, J., 2000. Microemulsions for topical delivery of 8-methoxsalen. J . Control. Rel. 69, 209-218.

Barthelemy, P., Farah, N., and Laforet, J. P. Transcutol - product profile. Product Information. 1-10. 1995. Gattefosse´.

Bayrak, Y., Iscan, M., 2005a. Studies on the phase behavior of the system non-ionic surfactant/alcohol/alkane/H2O. Colloids and Surfaces A-Physicochemical and Engineering Aspects, 268, 99-103.

Bayrak, Y., Iscan, M., 2005b. Phase behavior of oil/water/nonionic surfactant systems. J. Dispers. Sci. Technol. 26, 75-78.

Bisal, S., Bhattacharya, P.K., Moulik, S.P., 1990. Conductivity study of microemulsions - dependence of structural behavior of water oil systems on surfactant, cosurfactant, oil, and temperature. J. Phys. Chem. 94, 350-355.

Broto, F., Clausse, D., 1976. Study of freezing of supercooled water dispersed within emulsions by differential scanning calorimetry. J. Phys. C-Solid State Physics, 9, 4251-4257.

Chen, H., Chang, X., Weng, T., Zhao, X., Gao, Z., Yang, Y., Xu, H., Yang, X., 2004. A study of microemulsion systems for transdermal delivery of triptolide. J. Control. Rel. 98, 427-436.

Cho, Y.H., Kim, S., Bae, E.K., Mok, C.K., Park, J., 2008. Formulation of a cosurfactant-free O/W microemulsion using nonionic surfactant mixtures. J. Food Science. 73, E115-E121.

Clausse, M., Nicolas Morgantini, L., Zradba, A., Touraud, D., 1987a. Water/ionic surfactant/alkanol/hydrocarbon system: influence of certain constitution and composition parameters upon realms of existence and transport properties of microemulsion type media. In: Rosano,H.L., Clausse,M. (Eds.), Microemulsion systems, Marcel Dekker, 15-63.

Clausse, M., Nicolas Morgantini, L., Zradba, A., Touraud, D., 1987b. Water/sodium dodecylsulfate/l pentanol/N-dodecane microemulsions. Realms of existence and transport properties. In: Rosano,H.L., Clausse,M. (Eds.), Microemulsion systems, Marcel Dekker, 387-425.

Delgado-Charro, M.B., Iglesias-Vilas, G., Blanco-Mendez, J., Lopez-Quintela, M.A., Marty, J.P., Guy, R.H., 1997. Delivery of a hydrophilic solute through the skin from novel microemulsion systems. Eur. J. Pharm. Biopharm. 43, 37-42.

El Maghraby, G.M., 2008. Transdermal delivery of hydrocortisone from eucalyptus oil microemulsion: Effects of cosurfactants. Int. J. Pharm. 355, 285-292.

El-Laithy, H.M., 2003. Preparation and physicochemical characterization of dioctyl sodium sulfosuccinate (aerosol OT) microemulsion for oral drug delivery. AAPS Pharm. Sci. Tech. 4, E11.

Fanun, M., 2008. Phase behavior, transport, diffusion and structural parameters of nonionic surfactants microemulsions. J. Molecular Liq. 139, 14-22.

Farahmand, S., Maibach, H.I., 2009. Estimating skin permeability from physicochemical characteristics of drugs: A comparison between conventional models and an in vivo-based approach. Int. J. Pharm. 375, 41-47.

Florence, A.T., Tucker, I.G., Walters, K.A., 1983. Non-ionic surfactant structure and interactions with biological systems. Abstr. Papers Am. Chem. Soc. 186, 196-COLL.

Friberg, S.E., 1990. Micelles, microemulsions, liquid-crystals, and the structure of stratum-corneum lipids. J. Soc. Cosmet. Chem. 41, 155-171.

Friend, D.R., 1992. In vitro skin permeation techniques. J. Control. Rel. 18, 235-248.

Garti, N., Clement, V., Fanun, M., Leser, M.E., 2000. Some characteristics of sugar ester nonionic microemulsions in view of possible food applications. J. Agric. Food Chem. 48, 3945-3956.

Ghi, P.Y., Hill, D.J.T., Whittaker, A.K., 2002. PFG-NMR Measurements of the self-diffusion coefficients of water in equilibrium poly (HEMA-co-THFMA) hydrogels. Biomacromolecules. 3, 554-559.

Giustini, M., Palazzo, G., Colafemmina, G., DellaMonica, M., Giomini, M., Ceglie, A., 1996. Microstructure and dynamics of the water-in-oil CTAB/n-pentanol/n-hexane/water microemulsion: A spectroscopic and conductivity study. J Phys. Chem. 100, 3190-3198.

Golden, G.M., McKie, J.E., Potts, R.O., 1987. Role of stratum-corneum lipid fluidity in transdermal drug flux. J. Pharm. Sci. 76, 25-28.

Graf, A., Ablinger, E., Peters, S., Zimmer, A., Hook, S., Rades, T., 2008. Microemulsions containing lecithin and sugar-based surfactants: Nanoparticle templates for delivery of proteins and peptides. Int. J. Pharm. 350, 351-360.

Hou, M.J., Shah, D.O., 1987. Effects of the molecular-structure of the interface and continuous phase of solubilization of water in water oil microemulsions. Langmuir, 3, 1086-1096.

Krauel, K., Davies, N.M., Hook, S., Rades, T., 2005. Using different structure types of microemulsions for the preparation of poly(alkylcyanoacrylate) nanoparticles by interfacial polymerization. J. Control. Rel. 106, 76-87.

Lagourette, B., Peyrelasse, J., Boned, C., Clausse, M., 1979. Percolative conduction in microemulsion type Systems. Nature, 281, 60-62.

Langevin, D., 1988. Microemulsions. Acc. Chem. Res. 21, 255-260.

Lawrence, M.J., Rees, G.D., 2000. Microemulsion-based media as novel drug delivery systems. Adv. Drug Deliv. Rev. 45, 89-121.

Leichtnam, M.L., Rolland, H., Wüthrich, P., Guy, R.H., 2006a. Identification of penetration enhancers for testosterone transdermal delivery from spray formulations. J. Control. Rel. 113, 57-62.

Leichtnam, M.L., Rolland, H., Wüthrich, P., Guy, R.H., 2006b. Testosterone hormone replacement therapy: State-of-the-art and emerging technologies. Pharm. Res. 23, 1117-1132.

Leichtnam, M.L., Rolland, H., Wüthrich, P., Guy, R.H., 2006c. Formulation and evaluation of a testosterone transdermal spray. J. Pharm. Sci. 95, 1693-1702.

Leichtnam, M.L., Rolland, H. Wüthrich, P., Guy, R.H., 2006d. Enhancement of transdermal testosterone delivery by supersaturation. J. Pharm. Sci. 95, 2373-2379.

Libster, D., Aserin, A., Garti, N., 2006. A novel dispersion method comprising a nucleating agent solubilized in a microemulsion, in polymeric matrix: I. Dispersion method and polymer characterization. J. Colloid Interface Sci. 299, 172-181.

Lissant, K.J., 1974. Basic theory. In: Lissant,K.J. (Ed.), Emulsions and Emulsion Technology, Marcel Dekker Inc, New York, 4-10.

Liu, H.Z., Wang, Y.J., Lang, Y.Y., Yao, H.M., Dong, Y., Li, S.M., 2009. Bicontinuous cyclosporin A loaded water-AOT/Tween 85-isopropylmyristate microemulsion: structural characterization and dermal pharmacokinetics in vivo. J. Pharm. Sci 98, 1167-1176.

Lopez, A., Llinares, F., Cortell, C., Herraez, M., 2000. Comparative enhancer effects of Span (R) 20 with Tween (R) 20 and Azone (R) on the in vitro percutaneous penetration of compounds with different lipophilicities. Int. J. Pharm. 202, 133-140.

Malmstein, M., 1999. Microemulsion in pharmaceuticals. In: Kumar,P., Mittal,K.L. (Eds.), Handbook of Microemulsion: Science and Technology, Marcel Dekker, 755-772.

Mathew, C., Patanjali, P.K., Nabi, A., Maitra, A., 1988. On the concept of percolative conduction in water-in-oil microemulsions. Colloids Surf. 30, 253-263.

Mehta, S.K., Kaur, G., Bhasin, K.K., 2008. Incorporation of antitubercular drug isoniazid in pharmaceutically accepted microemulsion: Effect on microstructure and physical parameters. Pharm. Res. 25, 227-236.

Mitragotri, S., Edwards, D.A., Blankschtein, D., Langer, R., 1995. Mechanistic study of ultrasonically-enhanced transdermal drug-delivery. J. Pharm. Sci. 84, 697-706.

Okimoto, K., Rajewski, R.A., Stella, V.J., 1999. Release of testosterone from an osmotic pump tablet utilizing (SBE)7m-[beta]-cyclodextrin as both a solubilizing and an osmotic pump agent. J. Control. Rel. 58, 29-38.

Podlogar, F., Gagperlin, M., Tomsic, M., Jamnik, A., Rogac, M.B., 2004. Structural characterisation of water-Tween 40((R))/Imwitor 308((R))-isopropyl myristate microemulsions using different experimental methods. Int. J. Pharm. 276, 115-128.

Podlogar, F., Rogac, M.B., Gagperlin, M., 2005. The effect of internal structure of selected water-Tween 40 (R)-Imwitor 308 (R)-IPM microemulsions on ketoprofen release. Int. J. Pharm. 302, 68-77.

Rhee, Y.S., Choi, J.G., Park, E.S., Chi, S.C., 2001. Transdermal delivery of ketoprofen using microemulsions. Int. J. Pharm. 228, 161-170.

Safran, S.A., Webman, I., Grest, G.S., 1985. Percolation in interacting colloids. Phys. Rev. A, 32, 506-511.

Sekkat, N., Kalia, Y.N., Guy, R.H., 2004. Porcine ear skin as a model for the assessment of transdermal drug delivery to premature neonates. Pharm. Res. 21, 1390-1397.

Spernath, A., Aserin, A., Garti, N., 2006. Fully dilutable microemulsions embedded with phospholipids and stabilized by short-chain organic acids and polyols. J Colloid Interface Sci. 299, 900-909.

Stilbs, P., Rapacki, K., Lindman, B., 1983. Effect of alcohol cosurfactant length on microemulsion structure. J. Colloid Interface Sci. 95, 583-585.

Thevenin, M.A., Grossiord, J.L., Poelman, M.C., 1996. Sucrose esters/cosurfactant microemulsion systems for transdermal delivery: Assessment of bicontinuous structures. Int. J. Pharm. 137, 177-186.

Walters, K.A., Dugard, P.H., Florence, A.T., 1981. Non-ionic surfactants and gastric-mucosal transport of paraquat. J. Pharm. Pharmacol. 33, 207-213.

Williams, A.C., Barry, B.W., 2004. Penetration enhancers. Adv. Drug Del. Rev. 56, 603-618.

Williams,D.H., Fleming,I., 1996. Infrared Spectra. In: Williams,D.H., Fleming,I. (Eds.), Spectroscopic methods of analysis. Fifth edition. University Press, Cambridge, 28-62.

Winsor, P.A., 1948. Hydrotropy, solubilisation and related emulsification processes. J. Chem. Soc. Faraday Trans. 44, 376-398.

Yaghmur, A., Aserin, A., Tiunova, I., Garti, N., 2002. Sub-zero temperature behaviour of non-ionic microemulsions in the presence of propylene glycol by DSC. J. Therm. Analy. Calorim. 69, 163-177.

Yuan, J.S., Ansari, M., Samaan, M., Acosta, E.J., 2008. Linker-based lecithin microemulsions for transdermal delivery of lidocaine. Int. J. Pharm. 349, 130-143.

Zaslavsky, B.Y., Ossipov, N.N., Krivich, V.S., Baholdina, L.P., Rogozhin, S.V., 1978. Action of surface-active substances on biological membranes. 2. Hemolytic activity of non-ionic surfactants. Biochim. Biophys Acta, 507, 1-7.

Zhao, X., Liu, J.P., Zhang, X., Li, Y., 2006. Enhancement of transdermal delivery of theophylline using microemulsion vehicle. Int. J. Pharm. 327, 58-64.

Figure Legends

Figure 1 Phase diagram for the oleic acid/Tween20/Transcutol®/water system where the mixing ratio of Tween20 to Transcutol is 1:1. 1Φ represents the water-in-oil, bicontinuous phase and the oil-in-water microemulsion (one phase region); MΦ corresponds to multiple phase regions. W_m is the maximum amount of solubilised water, S_m is the amount of surfactant needed to obtain maximum water solubilisation and L20 is a dilution line where the initial oil concentration is 20% w/w.

Figure 2 Variation of the total monophasic region (A_T), the maximum amount of solubilised water (W_m), and the minimum amount of surfactant (S_m), needed to achieve maximum water solubilisation, as a function of Tween chain length.

Figure 3 Variation of the total monophasic region (A_T) as a function of the surfactant to co-surfactant ratio in the systems oleic acid/Tween20/Transcutol®/water.

Figure 4 Dependence of (a) electrical conductivity (σ), (b) (log σ)/t and (c) d(log σ)/dΦ, as a function of percentage water content (Φ) along the dilution line L20 for the system oleic acid/Tween20/Transcutol®/water presented in Figure 1.

Figure 5 DSC cooling curves (plotted as endothermic heat flow as a function of temperature) of pure water and of the selected microemulsions (see Table 2).

Figure 6 Relative diffusion coefficients (D/D_0) of water (o) and oil (Δ) of the selected microemulsions (see Table 2) as a function of water content.

Figure 7 Permeation of testosterone (1% w/v) from selected oleic acid/Tween20/Transcutol®/water microemulsions. The lines through the data are best fits to the appropriate solution of Fick's second law of diffusion (r^2 values were 0.71, 0.96, 0.97, 0.99, 0.90 and 0.99 for microemulsions A to F respectively).

Figure 8 Permeation of testosterone (at (a) 3%, w/v, and (b) 1% w/v) from microemulsion E. The lines through the data are best fits to the appropriate solution of Fick's second law of diffusion (r^2= 0.96 and 0.90, respectively).

Figure 1

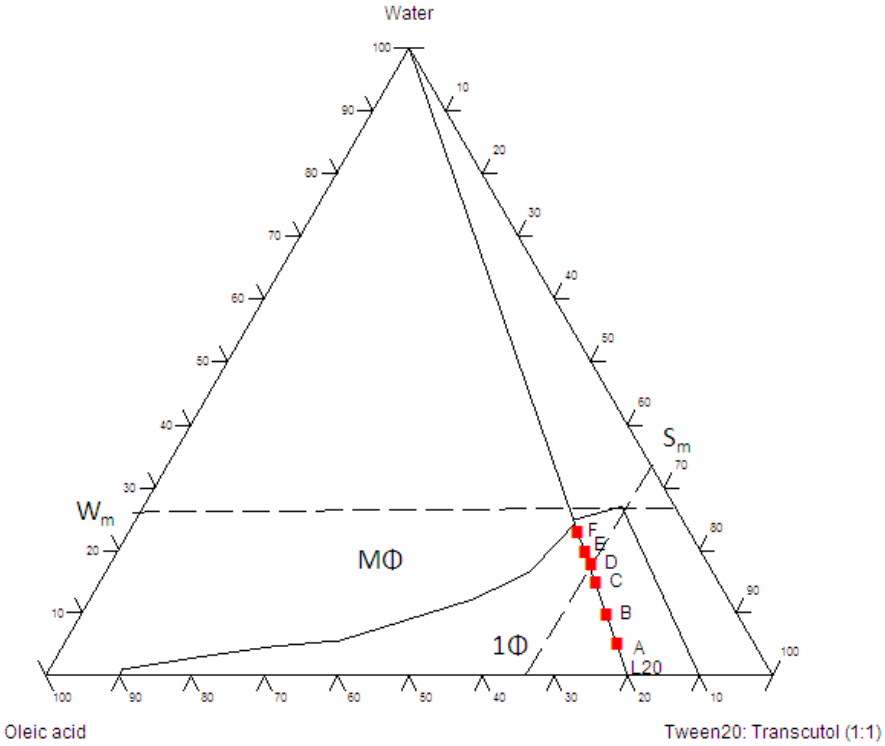
Water
Oleic acid
Tween20: Transcutol (1:1)
W_m
S_m
MΦ
1Φ
F
E
D
C
B
A
L20

Figure 2

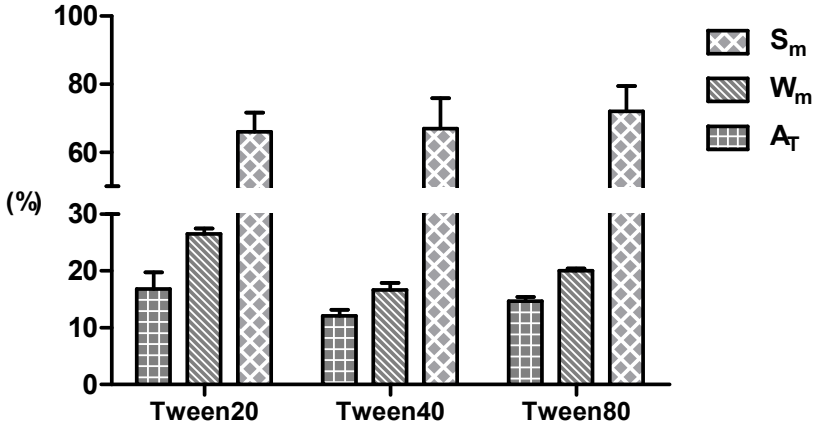

Figure 3

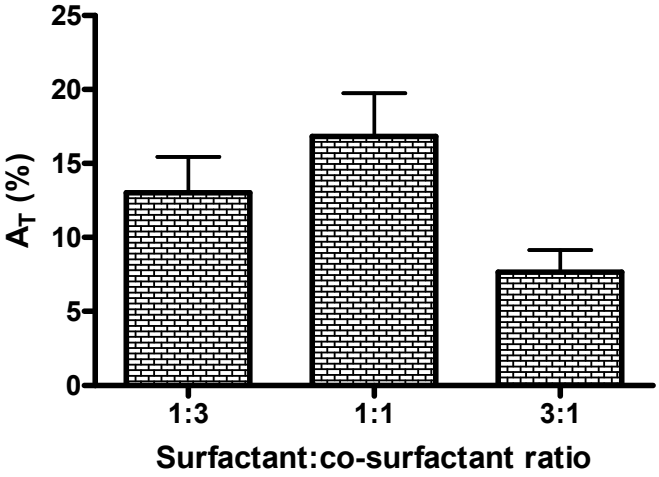

Figure 4

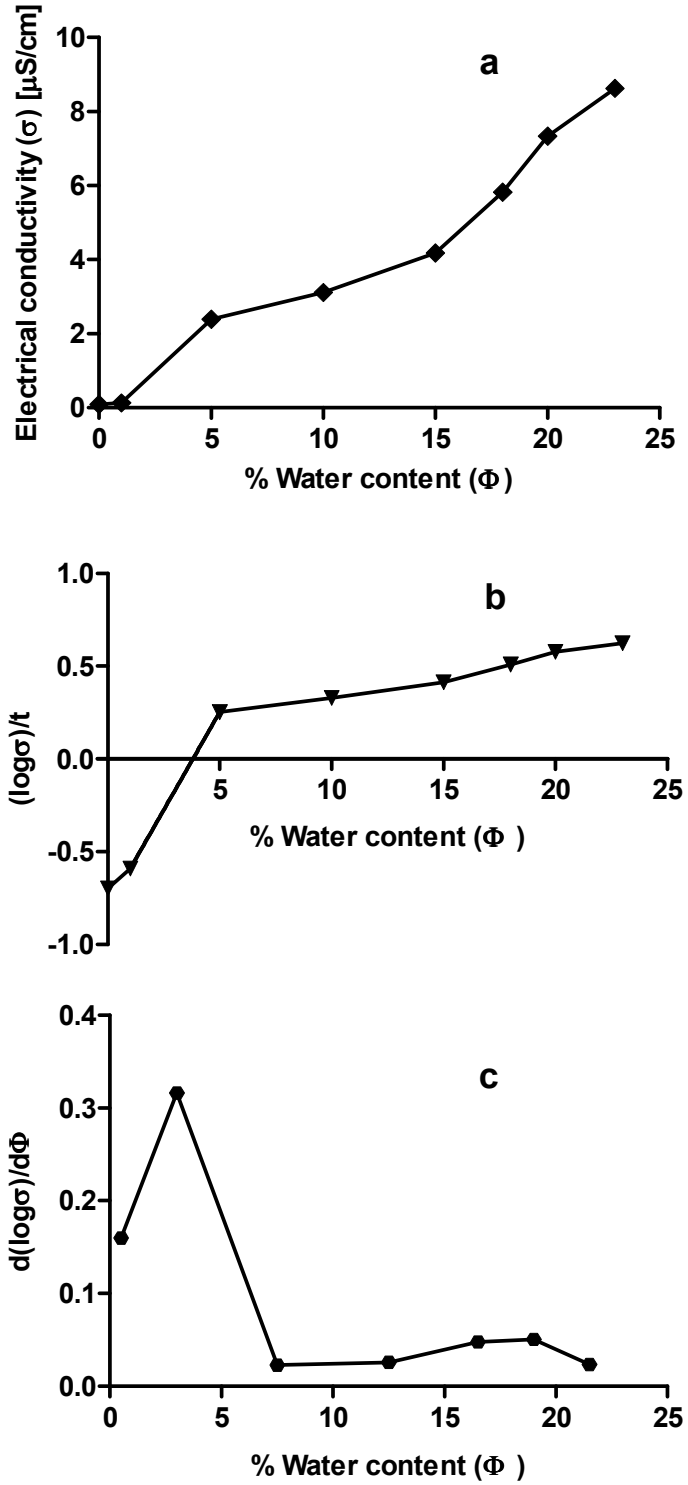
a
Electrical conductivity (σ) [µS/cm]
10
8
6
4
2
0
0
5
10
15
20
25
% Water content (Φ)
b
(logσ)/t
1.0
0.5
0.0
-0.5
-1.0
5
10
15
20
25
% Water content (Φ)
c
d(logσ)/dΦ
0.4
0.3
0.2
0.1
0.0
0
5
10
15
20
25
% Water content (Φ)

Figure 5

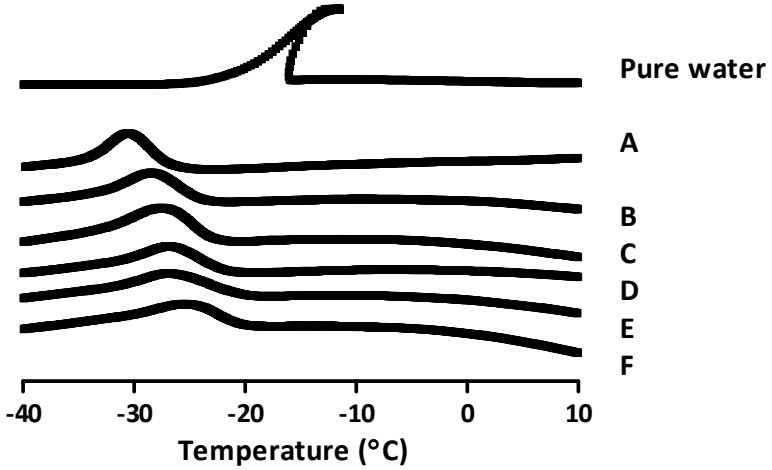

Figure 6

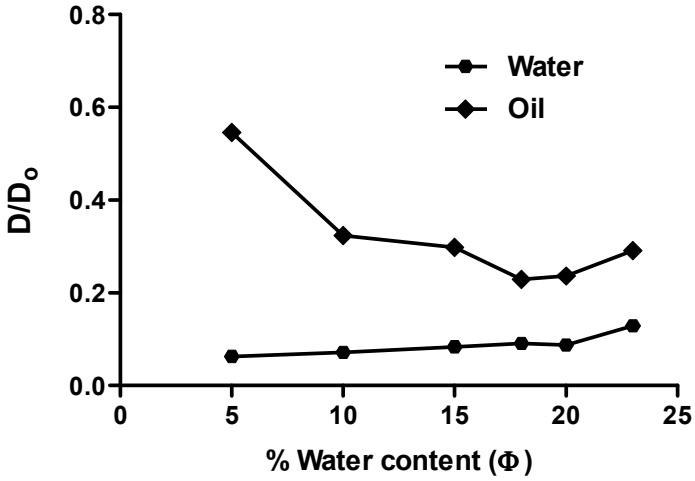

Figure 7

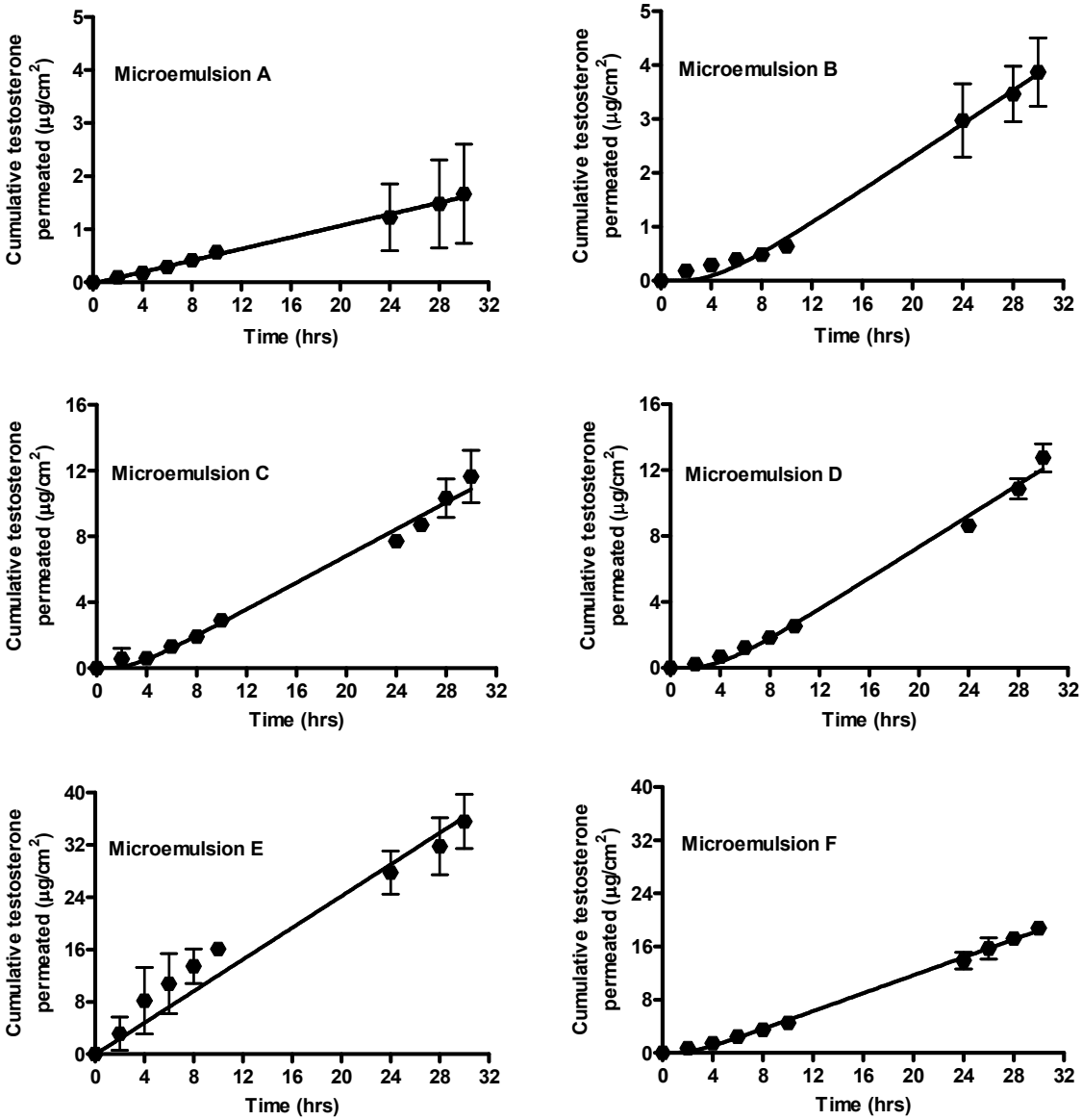
Microemulsion A
Microemulsion B
Microemulsion C
Microemulsion D
Microemulsion E
Microemulsion F
Cumulative testosterone permeated (µg/cm²)
Time (hrs)

Figure 8

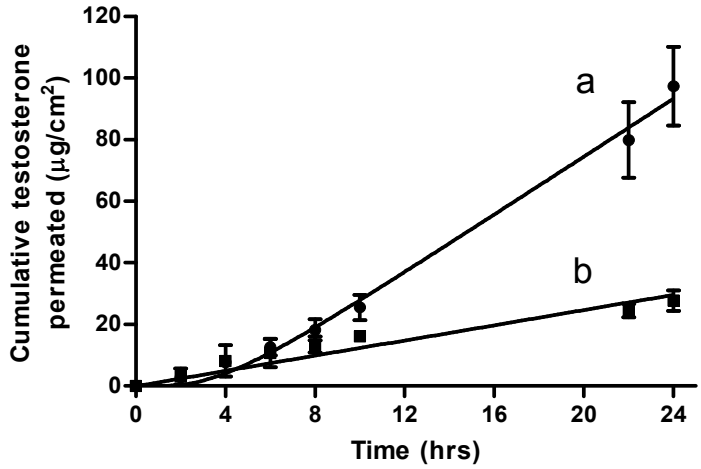
Cumulative testosterone permeated (μg/cm²)
120
100
80
60
40
20
0
0
4
8
12
16
20
24
Time (hrs)
a
b

Table 1: Dynamic light scattering characterization of selected microemulsions comprising oleic acid/Tween20/Transcutol®/water.

Microemulsion composition (%v/v) Oleic acid/Tween20/Transcutol®/Water	$Ø_w$	$Ø_o$	Z - average diameter (nm) ± S.D.	Polydispersity Index ± S.D.
70/14/14/2	0.27		10 ± 2	0.53 ± 0.31
50/22.5/22.5/5	0.46		13 ± 3	0.25 ± 0.19
30/30/30/10		0.90	13 ± 6	0.33 ± 0.13
10/35/35/20		0.79	10 ± 6	0.89 ± 0.14

Table 2: Selected microemulsion formulations (%v/v).

Components	Microemulsion					
	A	B	C	D	E	F
Oleic acid	19	18	17	16.2	16	15.4
Tween20	38	36	34	32.9	32	30.8
Transcutol®	38	36	34	32.9	32	30.8
Water	5	10	15	18	20	23

Table 3: Changes in the physical parameters of microemulsions (ME) after loading with drug (1% w/v).

ME	OH frequency (cm^{-1})		σ (μS/cm)		η (Pa.s)		pH	
	Unloaded	Loaded	Unloaded	Loaded	Unloaded	Loaded	Unloaded	Loaded
A	3449	3442	2.39 ± 0.16	2.35 ± 0.21	0.047 ± 0.011	0.036 ± 0.027	5.24 ± 0.01	5.30 ± 0.03
B	3436	3433	3.11 ± 0.27	3.63 ± 0.29	0.046 ± 0.012	0.049 ± 0.020	5.15 ± 0.04	5.14 ± 0.02
C	3434	3436	4.18 ± 0.64	5.04 ± 0.60	0.050 ± 0.016	0.062 ± 0.008	5.04 ± 0.03	4.97 ± 0.01
D	3426	3433	5.82 ± 0.53	6.35 ± 0.48	0.039 ± 0.018	0.062 ± 0.007	5.03 ± 0.03	4.97 ± 0.02
E*	3431	3434 *3434*	7.34 ± 0.23	7.20 ± 0.54 *6.68 ± 0.17*	0.037 ± 0.014	0.040 ± 0.017 *0.052 ± 0.016*	4.89 ± 0.02	4.90 ± 0.03 *4.92 ± 0.00*
F	3401	3402	8.63 ± 0.59	8.71 ± 0.32	0.061 ± 0.017	0.073 ± 0.037	4.45 ± 0.03	4.45 ± 0.01

*Values in italics represent the physical parameters of microemulsion E after loading with drug at 3% w/v.

Table 4: Testosterone partitioning (KH) and diffusivity (D/H^2) parameters, estimated permeability coefficients (k_p) and steady-state fluxes (J_{ss}) from different microemulsions (ME) containing oleic acid/Tween20/Transcutol®/water across porcine skin *in vitro*.

ME	10^3. KH (cm)	D/H^2 (hr^{-1})	10^5. k_p (cm/hr)	J_{ss} (μg. cm^{-2}. hr^{-1})
A	0.19 ± 0.03	0.03 ± 0.014	0.60 ± 0.31	0.06 ± 0.03
B	0.40 ± 0.05	0.03 ± 0.004	1.55 ± 0.23	0.15 ± 0.02
C	1.00 ± 0.60	0.06 ± 0.036	4.00 ± 0.90	0.41 ± 0.09
D	1.30 ± 0.18	0.04 ± 0.002	4.74 ± 0.32	0.47 ± 0.03
E*	2.70 ± 0.77 *3.93 ± 0.87*	0.05 ± 0.004 *0.04 ± 0.007*	11.4 ± 0.44 *15.4 ± 2.04*	1.40 ± 0.44 *4.63 ± 0.61*
F	1.13 ± 0.52	0.07± 0.026	7.68 ± 0.66	0.77 ± 0.05

*Values in italics are the results when microemulsion E contained the drug at a concentration of 3% w/v; in all other cases the drug concentration was 0.1%w/v.

Supplementary information

^{1}H-NMR chemical shifts of different functional groups of drug-free and drug-loaded microemulsions E and F.

Functional group	δ (ppm)		Δδ ($\delta^1 - \delta^0$)	δ (ppm)		Δδ ($\delta^3 - \delta^0$)
	ME F (δ^0)	ME F with 1% (w/v)drug (δ^1)		ME E (δ^0)	ME E with 3% (w/v) drug (δ^3)	
CH_3	0.855	0.888	0.033	0.962	0.986	0.024
CH_2	1.162	1.191	0.029	1.263	1.282	0.019
CH_2CH_2CO	1.543	1.571	0.028	1.645	1.663	0.018
CH_2CH	1.989	2.02	0.031	2.080	2.119	0.039
CH_2CO	2.208	2.23	0.022	2.308	2.324	0.016
OCH_2CH_2O	3.646	3.668	0.022	3.731	3.746	0.009
CH_2OCO	4.171	4.190	0.019	4.261	4.280	0.019
OH	4.653	4.652	-0.001	4.69	4.691	0.001
CH	5.287	5.318	0.031	5.393	5.420	0.027

^{13}C-NMR chemical shifts of oleic acid, Tween20 and Transcutol functional groups after incorporation of drug (1%, w/v) in ME F.

Oleic acid				Tween20				Transcutol			
Functional group	δ (ppm)		Δδ (δ^1- δ^0)	Functional group	δ (ppm)		Δδ (δ^1- δ^0)	Functional group	δ (ppm)		Δδ (δ^1- δ^0)
	ME F (δ^0)	ME F with 1% drug (δ^1)			ME F (δ^0)	ME F with 1% drug (δ^1)			ME F (δ^0)	ME F with 1% drug (δ^1)	
CH_3	14.117	14.806	0.689	CH_3	14.088	14.161	0.073	CH_3	14.843	14.916	0.073
CH_2	22.896 29.477 29.631 30.004	22.926 29.513 29.660 30.034	0.073 0.036 0.029 0.030	CH_2	22.896 29.477 29.631 30.004	22.926 29.513 29.660 30.034	0.073 0.036 0.029 0.030	C-OH	60.863	60.914	0.051
								C-O	70.067 72.375	70.126 72.441	0.029 0.066
CH_2CHCO	25.131	25.183	0.052	CH_2CH_2CO	25.754	25.791	0.037				
$CH_2C=C$	27.359	27.396	0.037	CH_2CO	34.086	34.130	0.044				
$CH_3CH_2CH_2$	32.188	32.225	0.037	C-OH	60.863	60.914	0.051				
CH_2CO	34.086	34.130	0.044	C-O	70.067 72.375	70.126 72.441	0.029 0.066				
C=C	129.725	129.871	0.146								
COOH	175.782	175.723	-0.049	C=O	175.782	175.733	-0.049				

[1]H-NMR spectra and assignment of peaks of microemulsion F.

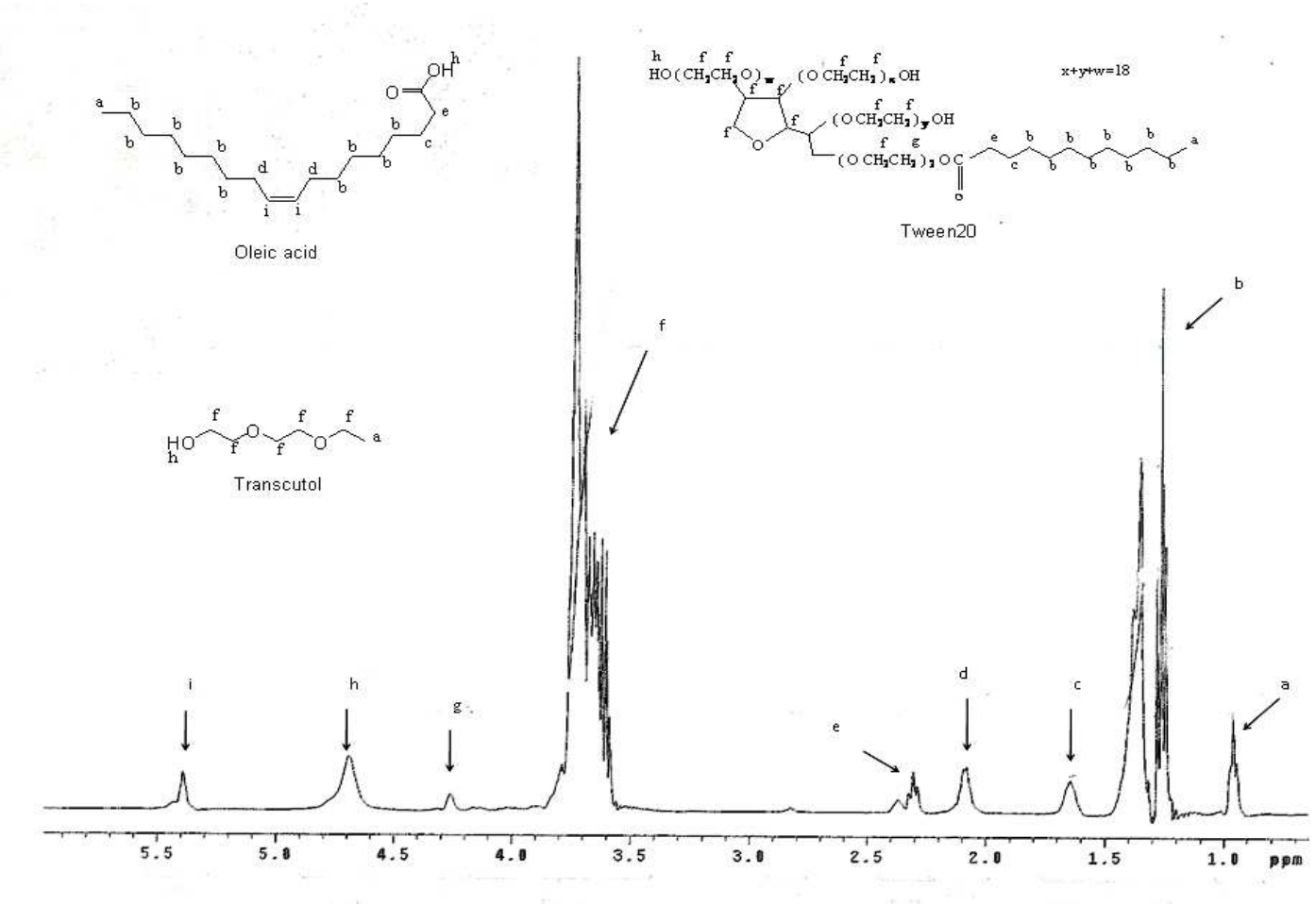

^{13}C-NMR spectra and assignment of peaks of microemulsion F.